

Epitaxially Self-Assembled Aggregates of Polyoxotungstate Nanocrystallites, $(\text{NH}_4)_3\text{PW}_{12}\text{O}_{40}$: Synthesis by Homogeneous Precipitation Using Decomposition of Urea

Takeru Ito,* Kei Inumaru,[†] and Makoto Misono[‡]

Department of Applied Chemistry, Graduate School of Engineering, The University of Tokyo, Hongo, Bunkyo-ku, Tokyo 113-8656, Japan

Received June 30, 2000. Revised Manuscript Received November 18, 2000

Microporous dodecahedral aggregates of a polyoxotungstate were synthesized by homogeneous precipitation from aqueous solution using hydrolysis of urea at 373 K ($\text{H}_3\text{PW}_{12}\text{O}_{40} + \frac{3}{2}(\text{NH}_2)_2\text{CO} + \frac{3}{2}\text{H}_2\text{O} \rightarrow (\text{NH}_4)_3\text{PW}_{12}\text{O}_{40} + \frac{3}{2}\text{CO}_2$). The aggregates isolated after various reaction periods were characterized by several methods such as high-resolution scanning electron microscopy, N_2 and Ar adsorption, X-ray and electron diffraction, and solid-state NMR. The formation process is also discussed. Each of these aggregates (0.3–5 μm in size) consisted of 5–10 nm nanocrystallites of $(\text{NH}_4)_3\text{PW}_{12}\text{O}_{40}$, which connected epitaxially (the same orientation of crystal planes), leaving pores between the nanocrystallites. With an increase in the reaction time, the initially formed spherical aggregates having micro- and mesopores gradually turned in to dodecahedral aggregates having only micropores and higher crystallinity. The dodecahedral aggregates obtained after 24 h were almost stoichiometric, $(\text{NH}_4)_3\text{PW}_{12}\text{O}_{40}$, according to ^{31}P NMR, and had essentially the same structure as those prepared previously by the titration method using NH_4HCO_3 aqueous solution. The origin of the micropores of the dodecahedra is believed to be the narrow spaces between the nanocrystallites (primary particles) of each aggregate.

Introduction

Self-assembly of fine nanoparticles is a topic of current interest as one of the promising processes for nanotechnology. Typical examples are “colloidal crystals”.¹ Recently, colloidal superlattices of metals^{2–4} or semiconductors^{5–9} have attracted much attention. Organic–inorganic hybrid nanocomposites^{10–12} and self-assembly of millimeter-scale components,¹³ as well as

novel porous materials¹⁴ and photonic crystals¹⁵ synthesized using colloidal arrays for template, are among the latest topics. As for colloidal particles, metallic and semiconducting nanocrystals exhibit a wide range of optical and electronic properties that are attributed to quantum confinement or surface effects of very fine particles.¹⁶ Such self-assembled aggregates have considerable possibility as tunable materials, in which these properties can be controlled by the type of clusters and the manner of their assembly.¹⁷

However, the self-assembly of nanoparticles is a subtle process, one difficult to control precisely. Only several systems with three-dimensional order have been reported,^{1,4,6–8} and aggregates in which each nanocrystal is crystallographically oriented in a regular way are rare.^{9,18} Therefore, the synthesis of various types of such aggregates and the elucidation of their formation mechanism are challenging objectives in nanotechnology. We

[†] Present address: Department of Applied Chemistry, Faculty of Engineering, Hiroshima University, 1-4-1 Kagamiyama, Higashi-Hiroshima 739-8257, Japan.

[‡] Present address: Department of Environmental Chemical Engineering, Kogakuin University, 1-24-2 Nishi-shinjuku, Shinjuku-ku, Tokyo 163-8677, Japan.

(1) (a) Luck, W.; Klier, M.; Wesslau, H. *Ber. Bunsen-Ges. Phys. Chem.* **1963**, *67*, 75. (b) Hiltner, P. A.; Krieger, I. M. *J. Phys. Chem.* **1969**, *73*, 2386. (c) Pieranski, P. *Contemp. Phys.* **1983**, *24*, 25. (d) Asher, S. A.; Holtz, J.; Liu, L.; Wu, Z.; *J. Am. Chem. Soc.* **1994**, *116*, 4997.

(2) Giersig, M.; Mulvaney, P. *Langmuir* **1993**, *9*, 3408.

(3) Brust, M.; Bethell, D.; Schiffrin, D. J.; Kiely, C. J. *Adv. Mater.* **1995**, *7*, 795.

(4) Whetten, R. L.; Khoury, J. T.; Alvarez, M. M.; Murthy, S.; Vezmar, I.; Wang, Z. L.; Stephens, P. W.; Cleveland, C. L.; Luedtke, W. D.; Landman, U. *Adv. Mater.* **1996**, *8*, 428.

(5) Bentzon, M. D.; van Wouterghem, J.; Mørup, S.; Thölen, A. *Philos. Mag. B* **1989**, *60*, 169.

(6) Motte, L.; Pileni, M. P. *J. Phys. Chem. B* **1998**, *102*, 4104.

(7) Spanhel, L.; Anderson, M. A. *J. Am. Chem. Soc.* **1991**, *113*, 2826.

(8) Murray, C. B.; Kagan, C. R.; Bawendi, M. G. *Science* **1995**, *270*, 1335.

(9) Vossmeier, T.; Reck, G.; Katsikas, L.; Haupt, E. T. K.; Schulz, B.; Weller, H. *Science* **1995**, *267*, 1476.

(10) Colvin, V. L.; Goldstein, A. N.; Alivisatos, A. P. *J. Am. Chem. Soc.* **1992**, *114*, 5221.

(11) Fendler, J. H.; Meldrum, F. C. *Adv. Mater.* **1995**, *7*, 607.

(12) Kimizuka, N.; Kunitake, T. *Adv. Mater.* **1996**, *8*, 89.

(13) (a) Bowden, N.; Terfort, A.; Carbeck, J.; Whitesides, G. M. *Science* **1997**, *276*, 233. (b) Tien, J.; Breen, T. L.; Whitesides, G. M. *J. Am. Chem. Soc.* **1998**, *120*, 12670.

(14) (a) Velev, O. D.; Jede, T. A.; Lobo, R. F.; Lenhoff, A. M. *Nature* **1997**, *389*, 447. (b) Holland, B. T.; Blanford, C. F.; Stein, A. *Science* **1998**, *281*, 538.

(15) (a) Wijnhoven, J. E. G. J.; Vos, W. L. *Science* **1998**, *281*, 802. (b) Zakhidov, A. A.; Baughman, R. H.; Iqbal, Z.; Cui, C.; Khayrullin, I.; Dantas, S. O.; Marti, J.; Ralchenko, V. G. *Science* **1998**, *282*, 897.

(16) Brus, L. E. *J. Chem. Phys.* **1983**, *79*, 5566; *J. Chem. Phys.* **1984**, *80*, 4403.

(17) (a) Kagan, C. R.; Murray, C. B.; Nirmal, M.; Bawendi, M. G. *Phys. Rev. Lett.* **1996**, *76*, 1517; **1996**, *76*, 3043. (b) Collier, C. P.; Saykally, R. J.; Shiang, J. J.; Henrichs, S. E.; Heath, J. R. *Science* **1997**, *277*, 1978.

previously reported nanocrystallites of polyoxotungstates which self-assembled into highly ordered, porous aggregates with high surface area.^{19–22} $(\text{NH}_4)_3\text{PW}_{12}\text{O}_{40}$ and $\text{Cs}_3\text{PW}_{12}\text{O}_{40}$ precipitated by a titration method (precipitation from an $\text{H}_3\text{PW}_{12}\text{O}_{40}$ aqueous solution by titration of an aqueous solution containing NH_4^+ or Cs^+) had different shapes, porosities, and crystallinities depending on the precipitation temperature and the alkali cations. Of particular interest is microporous $(\text{NH}_4)_3\text{PW}_{12}\text{O}_{40}$ precipitated at a high temperature.^{19,20} It had a regular dodecahedral shape and comprised nanocrystallites having the same orientation of crystal planes. Hence, each dodecahedral aggregate can be regarded as a microporous single crystal.

As for polyoxometalates (POMs) themselves, POMs belong to a rapidly growing field in inorganic chemistry.^{23–26} Recently, novel polyoxometalates with nanostructure have been reported. The structure of these polyoxometalates ranges from self-assembled monolayers²⁷ to colloidal particles,^{28–31} nanometer-ordered materials,^{32,33} thin films,³⁴ and microporous solids.^{35,36} In addition, polyoxometalates in the solid state have high potential as catalysts^{28,32a} or electronic^{34a} or magnetic^{34c} devices. As for solid catalysts, they have already many

practical applications owing to their strong acidities and unique redox properties.^{25,26}

In the present study, we synthesized novel porous aggregates of $(\text{NH}_4)_3\text{PW}_{12}\text{O}_{40}$ by homogeneous precipitation using the hydrolysis of urea ($(\text{NH}_2)_2\text{CO} + 2\text{H}^+ + \text{H}_2\text{O} \rightarrow 2\text{NH}_4^+ + \text{CO}_2$). In this method, NH_4^+ is produced, accompanied by CO_2 evolution uniformly in the solution, and after complete decomposition, nothing but NH_4^+ remains in the solution. Taking advantage of this, we also investigated the formation process of the porous aggregates, the elucidation of which will not only lead to precise control of their properties (shape, particle size, surface area, etc.) but will also help to increase the understanding of the self-assembly chemistry and colloid science. We adopted the method of homogeneous precipitation, because the system becomes much simpler than the titration method that we studied previously.²⁰ In the latter system, the concentration of solutions is not uniform and the process much depends on the rate of titration, stirring, aging time, etc. In contrast, in homogeneous precipitation, it is expected that the concentration of $\text{H}_3\text{PW}_{12}\text{O}_{40}$ is uniform and the rate of aggregate formation can be controlled exactly, so that we are able to examine the change with time of the structure of the aggregates and discuss key factors controlling the formation of aggregates.

Experimental Section

Materials. $\text{H}_3\text{PW}_{12}\text{O}_{40} \cdot n\text{H}_2\text{O}$ was supplied by Nippon Inorganic Color and Chemical Co., Ltd. and used after extraction with diethyl ether and recrystallization from water. This contained about 22 molecules of water of crystallization. Urea (Nacalai Tesque, Inc.) was recrystallized in a water–ethanol mixed solvent. 1-Propanol (Tokyo Chemical Industry Co., Ltd.) was used without further purification. The water used in this work was purified by Milli-RX12 α (Millipore Corp.).

Preparation Procedure of $(\text{NH}_4)_3\text{PW}_{12}\text{O}_{40}$ Aggregates. Aggregates of $(\text{NH}_4)_3\text{PW}_{12}\text{O}_{40}$ (denoted as “ NH_4 salt” herein-after) studied here were prepared by homogeneous precipitation as follows (the NH_4 salt usually does not contain water of crystallization). $\text{H}_3\text{PW}_{12}\text{O}_{40} \cdot 6\text{H}_2\text{O}$ was first prepared by evacuation of the hydrated $\text{H}_3\text{PW}_{12}\text{O}_{40}$ ($\sim 22\text{H}_2\text{O}$) at 323 K.³⁷ Then, a stoichiometric amount of urea (typically 1.5 mmol, 90 mg) was dissolved in an aqueous solution of $\text{H}_3\text{PW}_{12}\text{O}_{40} \cdot 6\text{H}_2\text{O}$ (typically 1 mmol, 40 mL of 0.025 M solution). The clear solution contained in a three-necked flask sealed by a balloon was heated in an oil bath kept at 373 K without stirring. The temperature of oil bath was elevated at ca. 4 K per minute, and it took about 30 min until the temperature reached 373 K and became constant. After heated for the prescribed period (3, 6, 12, or 24 h), the resulting suspension was quickly cooled to room temperature in a water bath. After centrifugation for 1 h, the supernatant was removed by decantation and the remaining precipitation was dispersed in water. This centrifugation–decantation procedure was repeated three times. Then, the precipitate was dispersed in water, and the resulting colloidal suspension was dried at 328 K with a vacuum rotary evaporator to obtain a white powder of the NH_4 salt. The yields were 35, 68, 85, and 92% for the reaction periods of 3, 6, 12, and 24 h, respectively. Hereafter, NH_4 salts prepared by homogeneous precipitation (HP) will be designated by HP- t , where t indicates the reaction period at 373 K.

The homogeneous precipitation of the NH_4 salt was also carried out in a 1-propanol–water mixed solvent (30 mL and 5 mL, respectively) at 373 K by heating for 24 h. This sample will be designated as HP-24h(PrOH– H_2O). 1-Propanol was

(18) (a) Park, G.-S.; Shindo, D.; Waseda, Y.; Sugimoto, T. *J. Colloid Interface Sci.* **1996**, *177*, 198. (b) Jongen, N.; Bowen, P.; Lemaitre, J.; Valmalette, J.-C.; Hofmann, H. *J. Colloid Interface Sci.* **2000**, *226*, 189.

(19) Inumaru, K.; Nakajima, H.; Ito, T.; Misono, M. *Chem. Lett.* **1996**, 559.

(20) Ito, T.; Inumaru, K.; Misono, M. *J. Phys. Chem. B* **1997**, *101*, 9958.

(21) (a) Ito, T.; Song, I.-K.; Inumaru, K.; Misono, M. *Chem. Lett.* **1997**, 727. (b) Inumaru, K.; Ito, T.; Misono, M. *Microporous Mesoporous Mater.* **1998**, *21*, 629.

(22) Inumaru, K.; Nakajima, H.; Hashimoto, M.; Misono, M. *Nippon Kagaku Kaishi* **1998**, 390.

(23) *Chem. Rev.* **1998**, *98*, 1. The entire issue is devoted to polyoxometalates.

(24) (a) Pope, M. T. *Heteropoly and Isopoly Oxometalates*; Springer: Berlin, 1983. (b) Day, V. W.; Klemperer, W. G. *Science* **1985**, *228*, 533.

(25) (a) Papaconstantinou, E. *Chem. Soc. Rev.* **1989**, *18*, 1. (b) Izumi, Y.; Urabe, K.; Onaka, M. *Zeolite, Clay, and Heteropoly Acid in Organic Reactions*; Kodansha: Tokyo; VCH: Weinheim, 1992. (c) Kozhevnikov, I. V. *Catal. Rev.-Sci. Eng.* **1995**, *37*, 311. (d) Moffat, J. B. *Appl. Catal. A* **1996**, *146*, 65.

(26) (a) Misono, M. *Catal. Rev.-Sci. Eng.* **1987**, *29*, 269; **1988**, *30*, 339. (b) Okuhara, T.; Mizuno, N.; Misono, M. *Adv. Catal.* **1996**, *41*, 113. (c) Mizuno, N.; Misono, M. *Chem. Rev.* **1998**, *98*, 199. (d) Mizuno, N.; Nozaki, C.; Kiyoto, I.; Misono, M. *J. Am. Chem. Soc.* **1998**, *120*, 9267.

(27) (a) Ge, M.; Zhong, B.; Klemperer, W. G.; Gewirth, A. A. *J. Am. Chem. Soc.* **1996**, *118*, 5812. (b) Song, I. K.; Kaba, M. S.; Barteau, M. A. *J. Phys. Chem.* **1996**, *100*, 17528.

(28) Aiken, J. D., III; Lin, Y.; Finke, R. G. *J. Mol. Catal. A* **1996**, *114*, 29.

(29) (a) Zamora, P. C.; Zukoski, C. F. *Langmuir* **1996**, *12*, 3541. (b) Ramakrishnan, S.; Zukoski, C. F. *J. Chem. Phys.* **2000**, *113*, 1237.

(30) (a) Koliadima, A.; Pérez-Maqueda, L. A.; Matijević, E. *Langmuir* **1997**, *13*, 3733. (b) Pérez-Maqueda, L. A.; Matijević, E. *Chem. Mater.* **1998**, *10*, 1430.

(31) Berndt, S.; Herein, D.; Zemlin, F.; Beckmann, E.; Weinberg, G.; Schütze, J.; Mestl, G.; Schlögl, R. *Ber. Bunsen-Ges. Phys. Chem.* **1998**, *102*, 763.

(32) (a) Kwon, T.; Tsigdinos, G. A.; Pinnavaia, T. J. *J. Am. Chem. Soc.* **1988**, *110*, 3653. (b) Drezdzon, M. A. *Inorg. Chem.* **1988**, *27*, 4628.

(33) (a) Stein, A.; Fendorf, M.; Jarvie, T. P.; Mueller, K. T.; Benesi, A. J.; Mallouk, T. E. *Chem. Mater.* **1995**, *7*, 304. (b) Taguchi, A.; Abe, T.; Iwamoto, M. *Adv. Mater.* **1998**, *10*, 667.

(34) (a) Moriguchi, I.; Hanai, K.; Hoshikuma, A.; Teraoka, Y.; Kagawa, S. *Chem. Lett.* **1994**, 691. (b) Keller, S. W.; Kim, H.-N.; Mallouk, T. E. *J. Am. Chem. Soc.* **1994**, *116*, 8817. (c) Clemente-León, M.; Mingotaud, C.; Agricole, B.; Gómez-García, C. J.; Coronado, E.; Delhaès, P. *Angew. Chem., Int. Ed. Engl.* **1997**, *36*, 1114.

(35) (a) Okuhara, T.; Nishimura, T.; Misono, M. *Chem. Lett.* **1995**, 155. (b) Yoshinaga, Y.; Seki, K.; Nakato, T.; Okuhara, T. *Angew. Chem., Int. Ed. Engl.* **1997**, *36*, 2833.

(36) Yamada, T.; Yoshinaga, Y.; Okuhara, T. *Bull. Chem. Soc. Jpn.* **1998**, *71*, 2727.

(37) Lee, K. Y.; Mizuno, N.; Okuhara, T.; Misono, M. *Bull. Chem. Soc. Jpn.* **1989**, *62*, 1731.

selected because it can dissolve $\text{H}_3\text{PW}_{12}\text{O}_{40}$ and has high boiling point.

In some cases, HP-24h samples were further processed in two different ways, pressing and grinding. For the former, HP-24h was pressed with Riken Power (P-1B) (Riken Seiki Co., Ltd.) at 200 kg cm^{-2} for 10 min. As for the latter, HP-24h was ground for 10 min using an agate mortar.

Characterization. Images by scanning electron microscopy (SEM) were obtained without sputtering with an S-900 (Hitachi) and a JSM-T20 (JEOL) instrument. Size distributions of aggregates were counted using several SEM images for each sample. N_2 adsorption isotherms were measured at 77 K by an ASAP-2000 (Micromeritics) after evacuation at 573 K for 2 h. Mesopore size distributions were calculated by the Barrett–Joyner–Halenda (BJH) method³⁸ using adsorption branches. In the case of HP-3h and HP-24h, Ar adsorption isotherms were recorded after evacuation at 573 K using an Omnisorp 100 (Beckman Coulter) for the micropore analysis by the Horváth–Kawazoe method.³⁹

Powder X-ray diffraction (XRD) patterns were recorded by an MXP³ diffractometer (Mac Science) using $\text{Cu K}\alpha$ irradiation without any prior pretreatment. The diffraction line widths were obtained after the subtraction of the instrumental width determined by the line width of well-crystallized NaCl powders. Electron diffraction (ED) measurements were carried out with a JEM-4000FX II microscope (JEOL) for HP-3h and HP-24h.

The average sizes of the nanocrystallites were calculated from the BET surface areas, assuming spherical shape. The lengths of ordered crystal structure were estimated by the Scherrer equation from the (222) line widths of XRD as in the previous study.²⁰ These values are denoted by $d(\text{BET})$ and $L(\text{XRD})$, respectively. The equations for calculations are

$$d(\text{BET}) = 6/S\rho$$

where S is the BET surface area of $(\text{NH}_4)_3\text{PW}_{12}\text{O}_{40}$ and ρ is the density of $(\text{NH}_4)_3\text{PW}_{12}\text{O}_{40}$ crystal ($6.08 \times 10^6 \text{ g m}^{-3}$), and

$$L(\text{XRD}) = \frac{0.9\lambda}{B \cos \theta}$$

where λ is the wavelength of $\text{Cu K}\alpha$ radiation, B is the calibrated half-width of the (222) peak in radian, and θ is the diffraction angle of the (222) peak in degrees.

Solid-state NMR spectra were recorded at room temperature with a CMX 300 Infinity (Chemagnetics) for HP-3h and HP-24h. The samples for the measurement were prepared in a small special glass cell^{40,41} by dehydration at 473 K under vacuum for 2 h and subsequent sealing in a vacuum. Single pulse excitations were used with MAS rate = ca. 3 kHz to obtain ^{31}P (121 MHz, without proton decoupling) and ^1H (300 MHz) NMR spectra.

Results

General Feature of Aggregate Formation by Homogeneous Precipitation. White precipitates started to form about 1 h after the temperature reached 373 K; the clear solution becoming cloudy. Then this cloudy solution turned into a thick white suspension within 10 min. As described below, spherical aggregates were initially formed and gradually turned into dodecahedral aggregates, which were more or less like microporous single crystals ($0.3\text{--}5 \mu\text{m}$ in size). Thus, these aggregates were essentially the same as those prepared

by the NH_4^+ titration method.²⁰ The dodecahedral aggregates prepared previously by the titration method will be called “Tit-dodec”, which indicates “titration-method dodecahedra”.

During the reaction, urea was gradually hydrolyzed into NH_4^+ and CO_2 :



As discussed below, urea decomposed completely after 12 h. But, with a short reaction time, unreacted $\text{H}_3\text{PW}_{12}\text{O}_{40}$ and urea partly deposit together with the aggregates of $(\text{NH}_4)_3\text{PW}_{12}\text{O}_{40}$. Especially when the centrifugation was insufficient, the aggregates were covered in thin layers of $\text{H}_3\text{PW}_{12}\text{O}_{40}$. It was confirmed by SEM that these thin layers were removed after washing by water, with little change in the shape of $(\text{NH}_4)_3\text{PW}_{12}\text{O}_{40}$ itself. The results and discussion hereafter deal with the thoroughly washed samples. TG-DTA data of these samples indicated only dehydration of physically absorbed water (below 423 K) and desorption of ammonia (decomposition of salts, above 623 K).

SEM Observation. Figure 1 shows SEM images of NH_4 salts prepared by homogeneous precipitation. After 3 h, nearly spherical aggregates of micron-order in size were formed, and they began to be dodecahedral after 6 h. For HP-6h, many aggregates smaller than 100 nm were coexistent.⁴² After 24 h, the aggregates became very regular dodecahedra. The size of HP-24h was $0.3\text{--}5 \mu\text{m}$.⁴³

Figure 2 shows the size distributions of the aggregates in number (solid) and weight (shaded). Both size distributions indicate that the average size of aggregates increased with the reaction time. The number-size distributions show that many small aggregates ($<0.8 \mu\text{m}$) present initially gradually decreased. The weight-size distributions demonstrate that the aggregates of $2.0\text{--}2.8 \mu\text{m}$ in size were dominant after 24 h. Besides, it is noted that the spherical aggregates larger than $2 \mu\text{m}$ in size were already formed after 3 h, as can be seen in Figures 1 and 2.

N_2 Adsorption. Figure 3 shows N_2 adsorption isotherms of the NH_4 salts. All isotherms showed sharp rises in the very low pressure range. In the isotherm of HP-3h, a gradual increase in the medium-pressure range and a small hysteresis loop were observed, indicating that HP-3h has both micro- and mesopores.⁴⁴ The size of these mesopores was not uniform and $2\text{--}10 \text{ nm}$ in diameter. With an increase in the reaction period, the slope in the medium-pressure range decreased and the hysteresis loop disappeared, demonstrating the decrease of mesopores. This was consistent with the mesopore size distributions. The isotherm of HP-24h had the typical shape of microporous materials.⁴⁴

BET surface areas of these aggregates are summarized in Table 1. With an increase in the reaction

(42) The number of those fine aggregates ($<0.4 \mu\text{m}$) was variable (50–90% in the size distribution of whole aggregates). It seems that a kind of transient state was observed after 6 h in Figure 1b. If one looks at the weight-size distribution, the changes with reaction time are almost monotonic (see Figure 2).

(43) Monodispersed aggregates are obtained with very dilute solutions both by the titration (*Chem. Lett.* **2000**, 830.) and homogeneous precipitation method.

(44) Gregg, S. J.; Sing, K. S. W. *Adsorption, Surface and Porosity*; Academic Press: London, **1982**.

(38) Barrett, E. P.; Joyner, L. G.; Halenda, P. P. *J. Am. Chem. Soc.* **1951**, *73*, 373.

(39) Horváth, G.; Kawazoe, K. *J. Chem. Eng. Jpn.* **1983**, *16*, 470.

(40) Uchida, S.; Inumaru, K.; Dereppe, J. M.; Misono, M. *Chem. Lett.* **1998**, 643.

(41) Uchida, S.; Inumaru, K.; Misono, M. *J. Phys. Chem. B* **2000**, *104*, 8108.

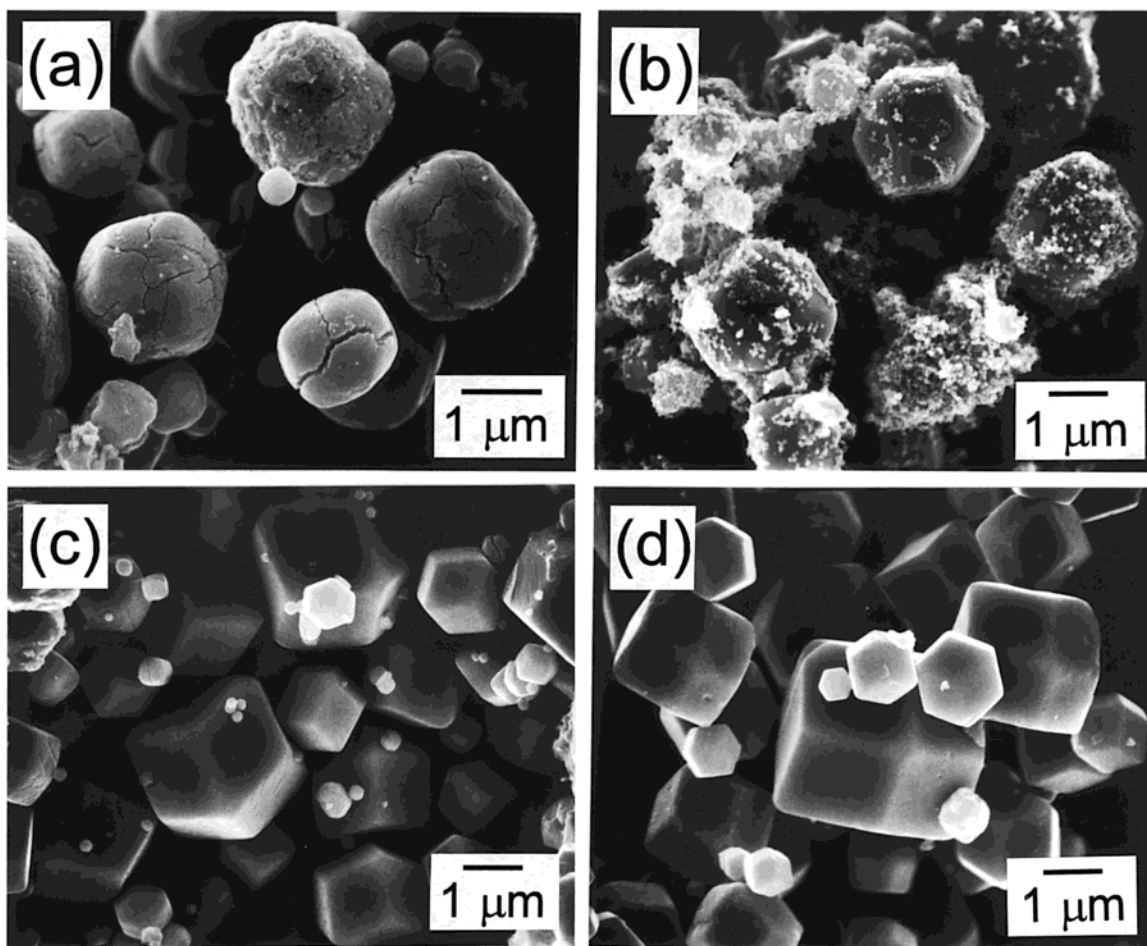


Figure 1. SEM images of $(\text{NH}_4)_3\text{PW}_{12}\text{O}_{40}$: (a) HP-3h, (b) HP-6h, (c) HP-12h, and (d) HP-24h. See note 42 for fine particles seen in b.

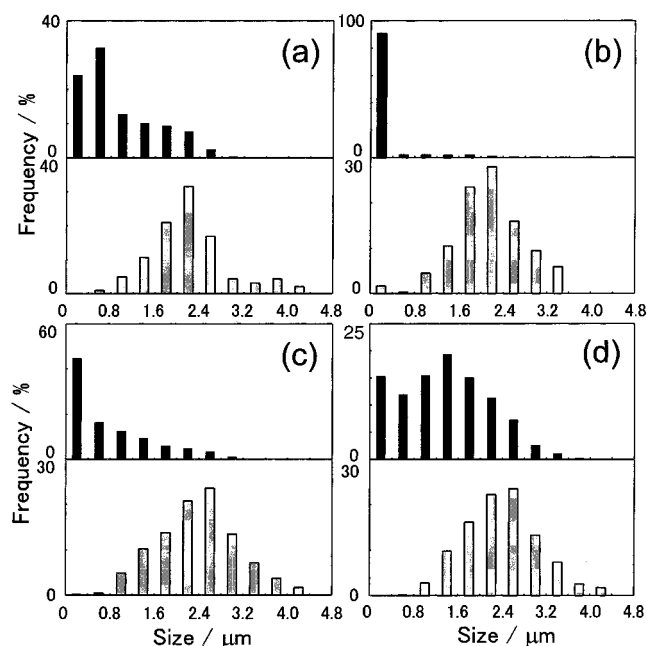


Figure 2. Size distributions in number (solid) and in weight (shaded) of $(\text{NH}_4)_3\text{PW}_{12}\text{O}_{40}$ aggregates: (a) HP-3h, (b) HP-6h, (c) HP-12h, and (d) HP-24h.

period, the BET surface area as well as N_2 adsorption amount decreased. For HP-3h and HP-24h, micropore size distributions were calculated by the Horváth–

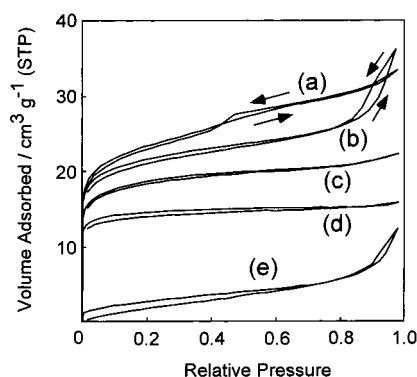


Figure 3. Isotherms of N_2 adsorption on $(\text{NH}_4)_3\text{PW}_{12}\text{O}_{40}$ aggregates at 77 K: (→) adsorption branch and (←) desorption branch for (a) HP-3h, (b) HP-6h, (c) HP-12h, (d) HP-24h, and (e) HP-24h ground for 10 min.

Kawazoe method from their Ar adsorption isotherms. The distributions were similar to each other, having a broad peak at 0.65 nm that tailed to 1.2 nm.

XRD and ED Measurement. As shown in Figure 4, NH_4 salts had a cubic crystal structure and all patterns were very similar. Table 1 shows the lengths of ordered crystal structure, $L(\text{XRD})$,²⁰ estimated from the XRD (222) line widths. $L(\text{XRD})$ increased as the reaction period was prolonged from 3 h (58 nm) to 6 h or longer (2.7×10^2 nm).

$L(\text{XRD})$ is the length in which the ordered crystal structure is coherent in terms of XRD, and $d(\text{BET})$ is

Table 1. Properties of $(\text{NH}_4)_3\text{PW}_{12}\text{O}_{40}$ Prepared by Homogeneous Precipitation

time ^a (h)	BET surface area (m ² g ⁻¹)	N ₂ adsorption amount (mmol g ⁻¹)	d(BET) ^b (nm)	L(XRD) ^c (nm)	L(XRD)/ d(BET)
3	81	1.5	12	58	4.8
6	74	1.6	13	2.7×10^2	21
12	64	1.0	15	2.6×10^2	17
24	49	0.71	20	2.6×10^2	13
Tit-dodec ²⁰	65	1.0	15	$81\text{--}1.5 \times 10^2$	5.4–10

^a Reaction period at 373 K. ^b The average size of the nanocrystallites calculated from the BET surface area, assuming spherical shape. ^c The length of the coherent ordered structure calculated by Scherrer's equation from (222) diffraction. See the text.

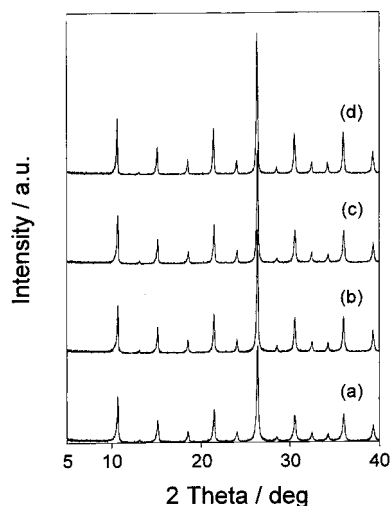


Figure 4. XRD powder patterns of $(\text{NH}_4)_3\text{PW}_{12}\text{O}_{40}$ aggregates: (a) HP-3h, (b) HP-6h, (c) HP-12h, and (d) HP-24h.

the average diameter of the nanocrystallites. Therefore, the ratio of $L(\text{XRD})/d(\text{BET})$ is an index of the extent of the "epitaxial self-assembly" as previously discussed for Tit-dodec samples.^{19,20} A large $L(\text{XRD})/d(\text{BET})$ ratio means that the number of nanocrystallites that connect epitaxially having sufficiently wide necks is large.²⁰ For example, the $L(\text{XRD})/d(\text{BET})$ of HP-24h was 13, indicating that the crystallographic coherence is at least 13 times greater than the size of nanocrystallite.

As for HP-3h and HP-24h, electron diffraction (ED) was measured. ED patterns exhibited discrete spots for both samples as in the case of Tit-dodec^{19,20} (not shown).

Solid-State NMR Measurement. ¹H and ³¹P NMR spectra of HP-3h and HP-24h are shown in Figure 5. Note that both samples contained no water molecules, as they had been dehydrated by evacuation at 473 K and sealed (Experimental Section). As shown in Figure 5a, a sharp and large peak at 5.4 ppm was observed together with a small broad peak at 9.8 ppm in the ¹H NMR spectrum of HP-3h. The former can be assigned to the proton of NH_4^+ ⁴⁵ and the latter to the residual acidic proton in $(\text{NH}_4)_x\text{H}_{3-x}\text{PW}_{12}\text{O}_{40}$. ³¹P NMR spectrum of HP-3h (Figure 5b) gave three peaks at -14.6, -13.3, and -11.9 ppm, which are assigned to polyanions having different numbers of protons (0, 1, and 2 protons) directly bound to polyanion, respectively, as discussed in the earlier work of the authors' group.⁴⁶ The ratio of polyanion and residual proton can be estimated by the peak areas (deconvoluted by Lorentzian function),⁴¹

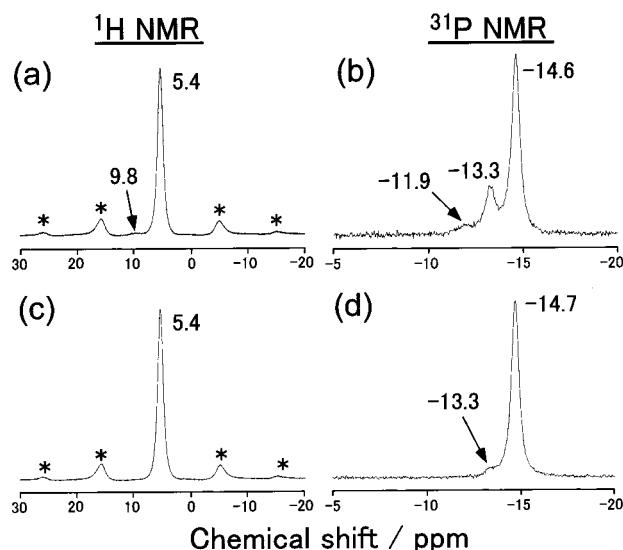


Figure 5. ¹H and ³¹P solid-state NMR spectra of HP-3h and HP-24h: (a) ¹H NMR of HP-3h, (b) ³¹P NMR of HP-3h, (c) ¹H NMR of HP-24h, and (d) ³¹P NMR of HP-24h. Asterisks attached to peaks denote spinning sidebands.

which indicated that the average formula of HP-3h is $(\text{NH}_4)_{2.7}\text{H}_{0.3}\text{PW}_{12}\text{O}_{40}$.

In the case of HP-24h, ¹H NMR spectrum (Figure 5c) gave only a sharp peak at 5.4 ppm, demonstrating that no residual proton exists to a detectable level. In ³¹P NMR spectrum (Figure 5d), a large peak at -14.7 ppm and a small peak at -13.3 ppm were observed. The peak ratio led to the formula of $(\text{NH}_4)_{2.98}\text{H}_{0.02}\text{PW}_{12}\text{O}_{40}$. This indicates that homogeneous precipitation can give a stoichiometric NH_4 salt ($\text{NH}_4^+:\text{PW}_{12}\text{O}_{40}^{3-} = 3:1$), although the titration method cannot.⁴⁷ This difference may be attributed to different heating periods between the two methods.

Fine Structure of the Surface of Aggregates. Figure 6 shows SEM images of greater magnification recorded for the surfaces of HP-3h and HP-24h. On the entire surfaces of HP-3h, fine nanocrystallites of $(\text{NH}_4)_3\text{PW}_{12}\text{O}_{40}$ (ca. 5–10 nm in size) were directly observed (Figure 6a). In some cases, aggregates had shallow cracks on the surface, and it was noted that similar arrays of fine nanocrystallites were present inside these cracks. To the contrary, nanocrystallites were not observed on the nearly flat surface of HP-24h (Figure 6b). However, fine nanocrystallites similar to those of HP-3h were clearly observed on the vertexes of HP-24h dodecahedra that were partly broken (Figure 6c).

Time Courses of Urea Decomposition. The quantity of residual urea during the precipitation reaction

(45) Vega, A. J.; Luz, Z. *J. Phys. Chem.* **1987**, *91*, 365.

(46) Okuhara, T.; Nishimura, T.; Watanabe, H.; Na, K.; Misono, M. *Acid-Base Catalysis II*; Kodansha: Tokyo; Elsevier: Amsterdam, 1994; p. 419.

(47) Soled, S.; Mieso, S.; McVicker, G.; Gates, W. E.; Gutierrez, A.; Paes, J. *Catal. Today* **1997**, *36*, 441.

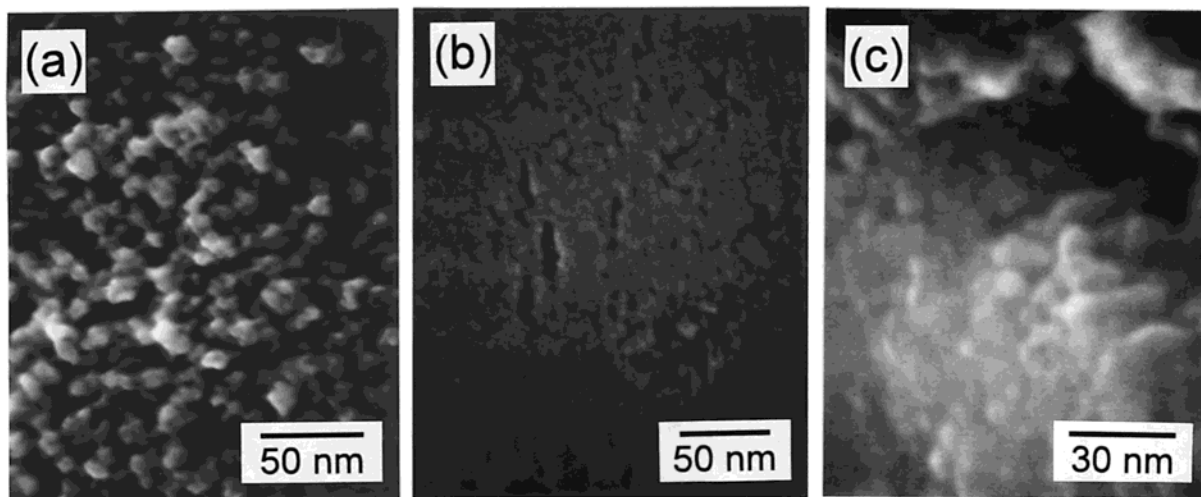


Figure 6. SEM images of the surface of $(\text{NH}_4)_3\text{PW}_{12}\text{O}_{40}$ aggregates at high magnification: (a) HP-3h, (b) HP-24h, and (c) partially broken vertexes of HP-24h.

was estimated by assuming that the quantity of urea decomposed was equal to the amount of $\text{H}_3\text{PW}_{12}\text{O}_{40}$ consumed (in 3:2 molar ratio). If one presumes that proton in the supernatant was derived from the dissociation of residual $\text{H}_3\text{PW}_{12}\text{O}_{40}$ ($\text{H}_3\text{PW}_{12}\text{O}_{40} \rightarrow 3\text{H}^+ + \text{PW}_{12}\text{O}_{40}^{3-}$), the fraction of the amount of $\text{H}_3\text{PW}_{12}\text{O}_{40}$ consumed, f , is calculated by the following formula,

$$f = \left(1 - \frac{n_{\text{H}}}{n_{\text{HPW}} \times 3} \right) \times 100 \quad n_{\text{H}} = 10^{-p} \times \frac{v}{1000}$$

where n_{HPW} is the initial amount of $\text{H}_3\text{PW}_{12}\text{O}_{40}$, n_{H} is the residual amount of proton estimated from pH [mol], and p and v are the pH and the volume of the supernatant, respectively.

The p and v values were 2.04, 100 mL; 2.28, 80 mL; 2.97, 60 mL; and 3.38, 80 mL for HP-3h, -6h, -12h, and -24h, respectively. The f values are calculated to be 69.1%, 85.2%, 97.8%, and 98.8% for HP-3h, -6h, -12h, and -24h, respectively. It is notable that f was already 97.8% after 12 h, indicating that urea was nearly completely hydrolyzed to NH_4^+ and CO_2 . This is consistent with the result obtained from the direct determination of residual urea,²² if the difference in the reaction temperature (373 K in this work and 383 K in ref 22) is taken into account.

Changes of Pore Structure by Compressing and Grinding. The isotherm of ground HP-24h had neither a large initial uptake nor a flat plateau in the higher pressure range (Figure 3e), indicating the disappearance of microporosity. After grinding, dodecahedra of HP-24h changed to agglomerates of ca. 100 nm particles with random shapes (Figure 7d). On the contrary, most dodecahedra survived after the pressing (Figure 7c), and the isotherm was essentially the same as those before pressing.

Effect of Solvent on the Formation of Dodecahedral Aggregates. Figure 7b shows that HP-24h($\text{PrOH-H}_2\text{O}$) was not dodecahedral aggregates but particles with various sizes and random shapes. Its isotherm with a hysteresis loop indicates the presence of mesopores as well as micropores. In terms of XRD, HP-24h($\text{PrOH-H}_2\text{O}$) was the same NH_4 salt of $\text{H}_3\text{PW}_{12}\text{O}_{40}$.

Discussion

The Structure of Dodecahedral NH_4 Salt Prepared by Homogeneous Precipitation. The structure of the dodecahedral NH_4 salt prepared by homogeneous precipitation for 24 h (HP-24h) had the following characteristics: (1) it is aggregates of $(\text{NH}_4)_3\text{PW}_{12}\text{O}_{40}$ nanocrystallites, (2) it is microporous, and (3) the nanocrystallites in each aggregate have the same orientation of crystal planes.

It is obvious that HP-24h is porous aggregates of nanocrystallites, since the outer surface area estimated from the SEM image (less than $3 \text{ m}^2 \text{ g}^{-1}$) was much smaller than the BET surface area ($49 \text{ m}^2 \text{ g}^{-1}$). HP-24h is regarded to be aggregates of fine particles whose size is on the order of $d(\text{BET})$ (ca. 20 nm). The SEM image (Figure 6c) directly shows fine crystallites of 5–10 nm, which are regarded as the components of the aggregates. One should remember that AFM observation showed the same surface structure for Tit-dodec,^{21a} which has essentially the same structural characteristics. Therefore, it is concluded that HP-24h is dodecahedral porous aggregates of fine nanocrystallites, essentially the same as in the case of Tit-dodec.^{19,20}

Up to now, the origin of micropores in NH_4 and Cs salts has been controversial: Gregg et al.⁴⁸ and the groups of Moffat⁴⁹ assumed that the micropores exist in the crystal structure itself, while Mizuno et al.⁵⁰ and Yamada et al.³⁶ proposed that they are spaces formed between the fine nanocrystallites, and Schlögl et al.³¹ supposed that they are polyanion vacancies in the case of $\text{Cs}_4\text{PMo}_{11}\text{VO}_{40}$. Since the intrinsic crystal structure of the NH_4 salt does not have micropores of 0.65–1.2 nm in diameter,²⁰ we consider it most probable that the micropores are the narrow spaces between the nanocrystallites, as discussed previously for $\text{Cs}_x\text{H}_{3-x}\text{PW}_{12}\text{O}_{40}$ ($x = 2.1, 3$).^{36,50} The drastic change of the microporosity with the ground HP-24h (from Figure 3d,e) may support this conclusion. We cannot exclude the possibility that

(48) Gregg, S. J.; Tayyab, M. M. *J. Chem. Soc., Faraday Trans. 1* **1978**, *74*, 348.

(49) (a) McMonagle, J. B.; Moffat, J. B. *J. Colloid Interface Sci.* **1984**, *101*, 479. (b) Taylor, D. B.; McMonagle, J. B.; Moffat, J. B. *J. Colloid Interface Sci.* **1985**, *108*, 278.

(50) Mizuno, N.; Misono, M. *Chem. Lett.* **1987**, 967.

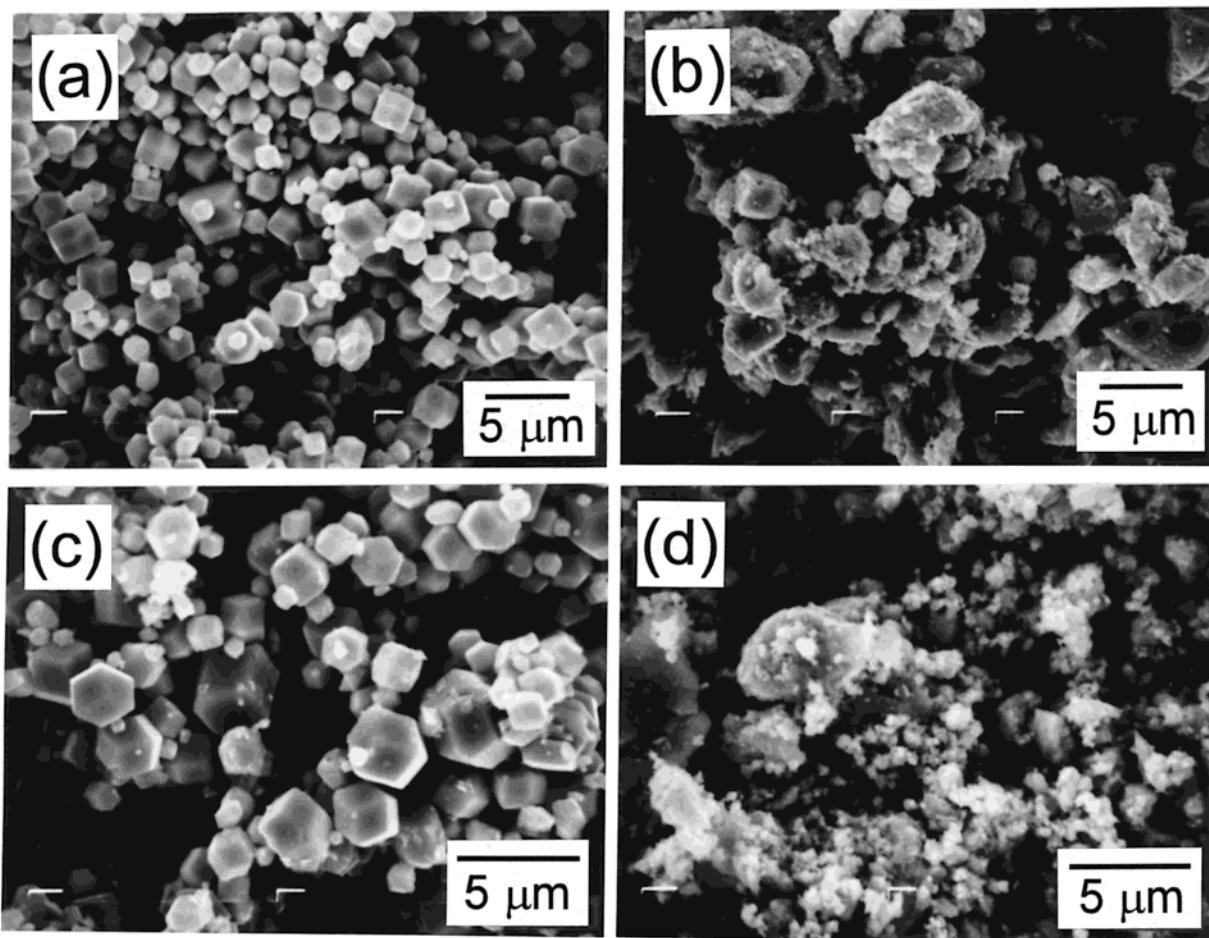


Figure 7. SEM images of HP-24h: (a) standard (see text), (b) prepared in a 1-propanol rich solvent, (c) pressed at 200 kg cm^{-2} for 10 min, and (d) ground for 10 min.

the structure formed at a certain stage of the aggregation in this study resembles the structure suggested by Schlögl et al.³¹

A comment on the epitaxial structure of HP-24h is useful at this point: the ED pattern of HP-24h exhibited discrete spots such as a single crystal, indicating that all nanocrystallites have the same crystal orientation, at least in the entire peripheral part, which was transparent to the electron beam. It may be reasonable to extend this statement to all the aggregates, that is, all nanocrystallites in each aggregate assembled with the same orientation of crystal planes. In addition, the $L(\text{XRD})$ value of $2.6 \times 10^2 \text{ nm}$ is 13 times larger than $d(\text{BET})$ ($= 20 \text{ nm}$). Since the possible largest value of $L(\text{XRD})$ is ca. 100 nm, owing to the principle of the measurement,⁵¹ the actual coherent length may be even greater. Therefore, at least 13 nanocrystallites connect epitaxially in HP-24h having sufficient width of necks. This means that the dodecahedral aggregates can be regarded as porous single crystals.

Finally, we speculate on the reason for the formation of the dodecahedral shape. XRD patterns (Figure 4) show that NH_4 salts have the same cubic crystal structure as $\text{H}_3\text{PW}_{12}\text{O}_{40}\cdot 6\text{H}_2\text{O}$.⁵² In the NH_4 salt, NH_4^+ cations replace $(\text{H}_2\text{O})_2\text{H}^+$ in the body-centered cubic

(bcc) structure of $\text{H}_3\text{PW}_{12}\text{O}_{40}\cdot 6\text{H}_2\text{O}$.^{20,52} Since $\{110\}$ and $\{100\}$ are the low-energy planes of the bcc structure,⁵³ the stable shape of the crystal is a rhombic dodecahedron surrounded by the $\{110\}$ planes or a cube surrounded by the $\{100\}$ planes. Namely, the external shape of the aggregates reflects the internal crystal structure as if the aggregates were single crystals. It is remarkable that the composition of HP-24h is almost stoichiometric according to ^{31}P NMR.

Formation Process of the Dodecahedral Aggregates. Note that large spherical aggregates ($> 2 \mu\text{m}$) are already formed after 3 h, indicating that spherical aggregates are rapidly formed at the initial stage (Figures 1a and 2a). These spheres (HP-3h) had mesopores in addition to micropores (Figure 3a), and their $L(\text{XRD})$ ($= 58 \text{ nm}$) is much smaller than that of HP-24h ($= 2.6 \times 10^2 \text{ nm}$), although the ED pattern showed discrete spots. Hence, the nanocrystallites of HP-3h have the same orientation of crystal planes, but the extent of epitaxial connection is low.

As the reaction period became longer, these aggregates gradually turned dodecahedral (Figure 1). At the same time, small aggregates ($< 0.8 \mu\text{m}$) decreased and disappeared after a certain period (Figure 2). In the meantime, the fraction of larger aggregates ($> 2 \mu\text{m}$) increased. These facts combined together lead to the

(51) *Characterization of Solid Catalysts (Japanese)*; Onishi, T., Ed.; Shokubai Koza vol. 3; Kodansha: Tokyo, 1985; p 120.

(52) Brown, G. M.; Noe-Spirlet, M.-R.; Busing, W. R.; Levy, H. A. *Acta Crystallogr., Sect. B* **1977**, *33*, 1038.

(53) Anderson, J. R. *Structure of Metallic Catalysts*; Academic Press: London, 1975.

conclusion that the small aggregates attach to the larger spherical aggregates and/or self-assemble with each other to form dodecahedral aggregates with an increase in the reaction period or a decrease in the concentration of NH_4^+ and $\text{PW}_{12}\text{O}_{40}^{3-}$. This conclusion is consistent with the fact that the surface of HP-24h turned flat (Figure 6b) and the edges became sharper (Figure 1b–d).

The increase in $L(\text{XRD})$ of HP-6h, -12h, and -24h indicates that the epitaxial connection of the spherical aggregates becomes tighter and thicker, which would decrease the larger voids (2–10 nm) brought about by irregular assembly of the nanocrystallites (5–10 nm). These voids may explain the presence of a small amount of mesopores.

In summary, the formation process is envisaged as follows: at the initial nucleation stage, spherical aggregates with meso- and micropores and low crystallinity are formed together with very fine particles. In the growth (aggregation) stage and as the precipitation reaction progresses, these spheres, in which the nanocrystallites loosely self-assemble, grow gradually into regular, microporous, highly crystalline, and rigid dodecahedra. Most of very fine precipitates probably attach to the surface of larger aggregates to grow the regular dodecahedra. Both the formation and the aggregation of nanocrystallites seem to be fast processes. On the contrary, the formation of the epitaxial connection and the growth of regular dodecahedral aggregates are slow, which may need partial dissolution and reprecipitation of $(\text{NH}_4)_3\text{PW}_{12}\text{O}_{40}$ nanocrystallites.

Factors Controlling the Formation of Dodecahedral Aggregates. In the case of the Cs salt which has lower solubility in water than the NH_4 salt, microporous aggregates of unidirectionally self-assembled nanocrystallites are formed only at high temperature (368 K), but these aggregates are spherical with a small $L(\text{XRD})$ value (=24 nm).²¹ This suggests that the lower solubility causes rapid precipitation, but aggregates formed have low epitaxy and crystallinity. The “dissolution and reprecipitation” process is probably very slow. Hence, the solubility of the salt seems to be a critical factor. The drastic effects of solvent on the morphology (Figures 7b) and porosity of the aggregates are consistent with this conclusion. Relevant here is literature showing that the NH_4 salt prepared by gas–solid reaction (without solvent) has neither micropores nor high surface area.^{49a}

Comparison with the Dodecahedral Aggregates Prepared by the NH_4^+ Titration Method. In the present study, by adopting the homogeneous precipitation method, we were able to study the formation

process of the dodecahedral porous aggregates of $(\text{NH}_4)\text{-PW}_{12}\text{O}_{40}$. Here the comparison between HP-24h and material prepared by the titration method (Tit-dodec)^{19,20} will be made. Both are dodecahedral aggregates of nanocrystallites with the same crystal orientation and microporous with micropores of similar size (0.56–1.3 nm (Tit-dodec) and 0.65–1.2 nm (HP-24h), respectively). The XRD and ED are also nearly the same. That is to say, the structures of HP-24h and Tit-dodec are essentially the same.

The following slight differences are noted between the two methods. First, the average size of Tit-dodec (0.7 μm) was smaller than that of HP-24h (1.4 μm), and the BET surface area (65 $\text{m}^2 \text{g}^{-1}$ for Tit-dodec) was larger (49 $\text{m}^2 \text{g}^{-1}$ for HP-24h). Second, the $L(\text{XRD})$ of Tit-dodec ($81\text{--}1.5 \times 10^2 \text{ nm}$) was a little smaller than that of HP-24h ($2.6 \times 10^2 \text{ nm}$) and so was $L(\text{XRD})/d(\text{BET})$ (5.4–10 for Tit-dodec, and 13 for HP-24h), which means that the epitaxial connection developed to a greater extent for HP-24h. These differences may be explained by the longer heating period and uniform precipitation and aggregation for homogeneous precipitation.

Conclusion

We were able to examine the formation process of epitaxially self-assembled $(\text{NH}_4)_3\text{PW}_{12}\text{O}_{40}$ nanocrystallites by employing a homogeneous precipitation method. The precipitation of nanocrystallites and their aggregation into spherical shape are fast processes. The increase in the reaction time made the aggregates dodecahedral, microporous (without mesopore), and highly crystalline through relocation and rearrangement of nanocrystallites, probably by “partial dissolution and reprecipitation”. During this period, the epitaxial connection of the nanocrystallites grows and the mesopores decreases. The micropores are believed to be narrow spaces between the nanocrystallites. The dodecahedra obtained after 24 h were essentially the same as those prepared by the titration method. The solubility of the salt seems to be a decisive factor for the formation of the dodecahedral aggregates with microporosity.

Acknowledgment. This work was supported in part by a Grant-in-Aid in a Priority Area from the Ministry of Education, Science, Sports and Culture. T.I. is grateful to the Research Fellowships of the Japan Society for the Promotion of Science for Young Scientists. Ms. Sayaka Uchida is specially acknowledged for NMR measurement and Professor Noritaka Mizuno for helpful discussion.

CM000541N